14th International Conference on Structural Safety and Reliability - ICOSSAR'25
1-6 June, 2025 - Los Angeles California, USA
R. Ghanem, E. Johnson, S. Masri and A. Olivier (Eds)

PHYSICS-BASED PARAMETERIZED FRAGILITY MODELS FOR COASTAL RESIDENTIAL BUILDINGS CONSIDERING THE EFFECTS OF NEIGHBORING STRUCTURES

JAINISH MAHESHBHAI PATEL[1] AND JAMIE ELLEN PADGETT[2]

[1]Rice University
Houston, TX 77005, United States
Jainish.patel@rice.edu

[2]Rice University
Houston, TX 77005, United States
Jamie.padgett@rice.edu

Key words: residential buildings, neighboring structures, topology-aware parameterized fragility model, active learning, storm surge and waves

Abstract. Coastal infrastructure continues to suffer widespread damage from hurricane events leading to significant economic losses. Among the most vulnerable structures are wood-framed residential buildings, which have been repeatedly exposed to storm surge and wave actions in past events. Acknowledging this vulnerability, researchers have developed fragility models using physics-based simulations to assess the damage incurred by these buildings in coastal communities. However, the influence of neighboring structures in residential building portfolios has been overlooked in current physics-based fragility derivation procedures, despite past hurricane-induced storm surge events highlighting their potential impact on demand modification across the portfolio due to wave deformation phenomena. This oversight limits the models' accurate representation of portfolio performance in risk assessments. To address this gap, this study develops closed-form parameterized fragility functions for residential buildings that account for the effects of neighboring structures. Using computational fluid dynamics (CFD) simulations, this study captures the modification in demand exerted by nearby buildings by incorporating multiple structures into the numerical analysis domain. To overcome the high computational cost of full-scale CFD simulations, an active learning algorithm is leveraged to guide the sample selection process, focusing only on critical parameter combinations of hazard and structural properties. Findings reveal that the probability of building failure varies based on proximity to the coastline, with structures closer to the coast being more directly affected and those farther inland experiencing greater influence from neighboring structures. These fragility models enhance the accuracy of portfolio-level risk assessments while enabling rapid vulnerability evaluations through their closed-form functional relationships. The improved regional vulnerability estimates are expected to better inform risk mitigation decisions for structures as well as inform the design of portfolio layouts that minimize the demands imposed by neighboring buildings.

1 INTRODUCTION

Hurricanes pose a substantial threat to coastal infrastructure, and have caused widespread damage during past hurricane occurrences [1]. During these events, structures are exposed to multi-hazard stressors, such as storm surge, wave loads, wind, and rainfall. Specifically, recent hurricane occurrences have highlighted the vulnerability of coastal wood-framed residential buildings to storm surge and wave loads, resulting in significant damages [2, 3]. Recognizing the risk associated with this critical component of coastal infrastructure to storm surge and wave actions, researchers have developed fragility models to quantify their conditional reliability. Existing building fragility models for storm surge and wave hazard, based on their derivation process, are broadly categorized into two approaches: (i) empirical fragility models, derived from field survey data collected from past hurricane events [4, 5, 6], and (ii) physics-based fragility models, derived using simulated data from physics-based numerical models [7]. While empirical fragility models provide useful insights into damage trends and the relative importance of key parameters, their transferability is limited, as they are derived from damage datasets of a specific region or hurricane event that may not reflect varying characteristics of the hazard elsewhere [8, 9]. Conversely, physics-based fragility models are typically derived using parameterized hazard scenarios, enabling them to account for uncertainties in hazard characteristics and making them well-suited for risk assessment studies across different regions.

The development of physics-based fragility models for storm surge and wave actions relies on numerical simulations to accurately estimate the loads on the structure since storm surge and wave loads represent highly nonlinear phenomena, and the analytically approximated formulas may not adequately capture the nonlinear action of wave loads [10]. The advancements in computational fluid dynamics (CFD) simulation enables accurate capture of such effects, thereby making them reliable tool for estimating loads on structures subjected to storm surge and wave actions [11, 12]. Subsequently, the physics-based fragility derivation process typically involves performing CFD simulations for a representative single structure subjected to varying storm surges and wave loads [7]. However, much of the coastal residential building infrastructure in the United States is densely arranged. Therefore, when storm surge and wave loads propagate from the coast to further inland, the loads exerted across different structures within the portfolio are likely to be modified due to neighboring structures. Observed damages from past hurricane events suggest a strong presence of demand modification effects, where different structures within the coastal residential building portfolio experienced different levels of damages even when accounting for variation in design details [4, 6, 13, 14]. These findings underscore the need to incorporate the influence of neighboring structures to obtain refined risk estimates.

Applying existing fragility models to dense portfolio configurations requires precise local estimates of hazard intensity measures to ensure accurate vulnerability estimates. However, the extent of hazard intensity modification has been found to vary with the properties of the waves and the configuration of neighboring structures, as highlighted by several experimental studies investigating the effects of neighboring structures under different surge and wave conditions [15, 16, 17, 18, 19]. Consequently, experimental studies are often not feasible for testing larger combinations of different surge and wave conditions needed for probabilistic analysis due to their prohibitive costs. An alternative approach is to use high fidelity numerical hazard simulations to obtain modified intensity measures considering their interactions with buildings

and other structures. However, repetitive analyses required for probabilistic assessment through various combinations of hazard intensity measure parameters, coupled with unique portfolio characteristics across various regions, renders such hazard simulations challenging due to their substantial computational costs [2, 6].

To incorporate the modification effects exerted by neighboring structures in risk assessments, a methodology is presented in this paper to develop a new set of "topology-aware" parameterized fragility models that incorporate the effects of neighboring structures by including the modified demand exerted by neighboring structures through physics-based simulations. The modified demand due to neighboring structures is estimated by leveraging physics-based numerical CFD analyses, including multiple structures within the fluid domain. Adding multiple structures within the fluid domain increases the computational expenses; however, an active learning strategy is embedded in the fragility derivation process to alleviate the computational burden [20]. Active learning methods have been found useful in reducing computational burden by steering the sample selection such that only the most critical samples are selected for the analysis [21].

For simplicity and illustrative purposes, this paper presents the proposed "topology-aware" parameterized fragility model derivation process for a single component of residential buildings, i.e., windows. The subsequent sections provide a detailed explanation of each step involved in deriving parameterized fragility models that incorporate the effects of neighboring structures.

2 PHYSICS-BASED TOPOLOGY-AWARE PARAMETERIZED FRAGILITY MODEL DERIVATION CONSIDERING THE EFFECTS OF NEIGHBORING STRUCTURES

The derivation of the topology-aware parameterized fragility model, which incorporates the effects of neighboring structures, begins with identifying parameters related to hazard intensity measures, layout and planar geometrical parameters of buildings, and individual building characteristics. The hazard intensity measure includes storm surge and wave parameters. For illustration purposes, only regular nonbreaking waves are considered in this study. The storm surge with regular nonbreaking waves can be described uniquely with the following parameters: storm surge (S), wave height (H_w), wave period (T_w), current (U), and wavelength (L_w). The parameter ranges for each hazard intensity measure considered in this study are presented in Table 1. These ranges are derived from the respective parameter bounds specified in [11] and have been slightly modified to include wider parameter ranges from numerical simulation results for different historical hurricane events [22].

The layout and planar geometrical parameters describe the spatial configuration of buildings with their neighboring buildings. The objective of including this set of parameters is to capture the effects of neighboring structures on demand modification. The demand modification caused by neighboring structures can be classified into two categories: structural shielding and channeling [19]. Structural shielding corresponds to a reduction in the hydraulic load, whereas channeling effects correspond to an increase in the hydraulic demand, both due to the presence of neighboring structures on the upstream side of the structure. Past studies have demonstrated that such effects can be captured by using a "three-structure layout": two structures in the upstream row (alternatively referred as row 1 here) and one structure on the downstream side

(row 2). Therefore, this study considers different spatial configurations of three structure layouts to quantify the effect of neighboring structures on demand modification and include them in the parameterized fragility model derivation (Figure 1). As shown in Figure 1, buildings 1 and 2 are in the first row (unobstructed by any upstream structure), while building 3 is in the second row. Accordingly, the layout and geometrical building parameters included in this study are the width and length of each building ($b_1, l_1, b_2, l_2, b_3, l_3$), transverse spacing between building 1 and building 2 (d_Y), relative offset between building 1 and building 3 (e), and closest distance between building rows (d_X). The ranges for each layout and geometrical parameters are determined by analyzing the building footprints (dataset available from [23]) for coastal building portfolios of the following coastal regions: Galveston Beach, TX, Fort Myers Beach, FL, and Ortley Beach, NJ. Table 1 summarizes different parameters and their ranges considered in this study.

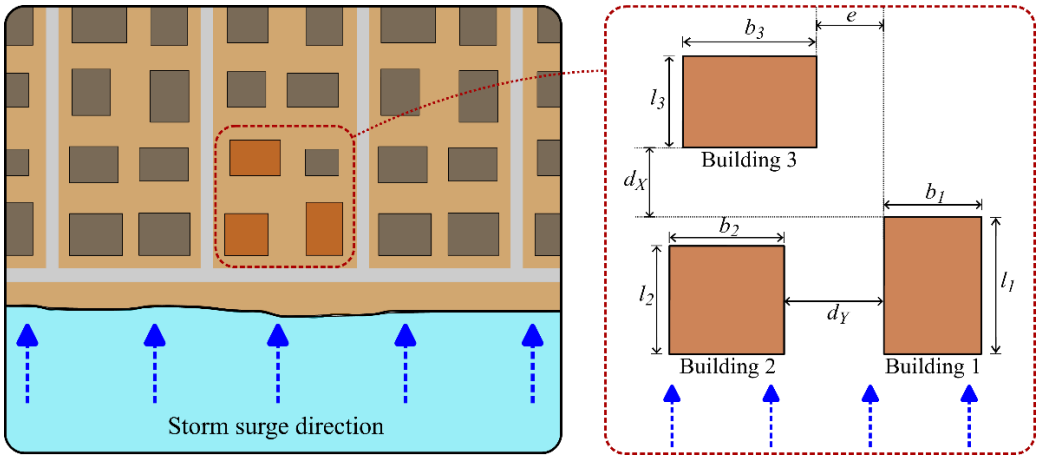

Figure 1: Schematic representation of typical coastal residential building portfolio and the "three-structure layout" considered in this study to examine the effects of neighboring structures on demand modification under storm surge and wave hazards

The individual building characteristics include parameters such as properties of structural (different types of connections used in the building) and nonstructural components (windows and doors), height of the lowest horizontal structural member (LHSM), and foundation type. While the development of fragility models can also incorporate different ranges of individual building characteristics, this study focuses on quantifying the effects of neighboring structures in deriving a parameterized fragility model. Therefore, to simplify the process, several assumptions were made in this study related to building characteristics. The buildings are assumed to be elevated with an LHSM height of 2.5 m above ground, and the fragility derivation is limited to the failure of a single building component—windows. The windows are assumed to be located on the front face of the building between the bounds of 1.1 m from the LHSM to 2.3 m, which is termed a "window zone" throughout this paper. The lateral resistance capacity of the window is treated as deterministic based on previous studies that report a mean resistance value of 3.35 kPa [7, 24]. Consequently, the limit state equation for window failure can be formulated as:

$$\mathcal{G} = 3.35 - \mathcal{D}_{max} \tag{1}$$

where, $\mathcal{D}_{max}$ is the maximum imposed hydraulic pressure (or modified pressure due to neighboring buildings) observed within the "window zone" due to storm surge and wave loads. The value of $\mathcal{G} \leq 0$ corresponds to failure, whereas $\mathcal{G} > 0$ represents survival of the respective building component. As evidenced in Equation 1, evaluating the limit state equation requires estimating $\mathcal{D}_{max}$ while accounting for the effects of neighboring structures. This is achieved through numerical CFD simulation, as outlined next.

Table 1: Ranges of hazard intensity measures, spatial layout and geometrical parameters

Parameter	Lower bound	Upper bound
Hazard intensity measures:		
Storm surge, S (m)	1.0	8.0
Wave height, H_w (m)	0.2	$0.65S$
Wave period, T_w (m)	3.0	10.0
Current, U (m)	0	1.5
Wave length, L_w (m)	7.5	80.0
Spatial layout and planar geometrical parameters:		
Width of building 1, b_1 (m)	5.0	30.0
Length of building 1, l_1 (m)	5.0	30.0
Width of building 2, b_2 (m)	5.0	30.0
Length of building 2, l_2 (m)	5.0	30.0
Width of building 3, b_3 (m)	5.0	30.0
Length of building 3, l_3 (m)	5.0	30.0
Offset distance, e (m)	$-b_1$	$d_Y + b_2 - b_3$
Closest distance between building rows, d_X (m)	3.0	50.0
Transverse spacing between building 1 and 2, d_Y (m)	3.0	50.0

2.1 Numerical model

The numerical model to perform CFD analysis is developed using commercial software *LS-Dyna* [25]. Figure 2 shows the CFD model domain consisting of three full-scale rectangular buildings. The entire domain of the model consists of solid hexahedral elements. The waves are generated at the inlet boundary by specifying the imposed velocity of all nodes based on Fenton's wave theory to generate desired waves [26]. The side boundaries are assigned free-slip conditions since no physical boundary exists along these surfaces. The bottom surface is assigned a no-slip condition to represent the ground surface. Non-reflecting elements are used at the outlet to absorb the waves. The water-air interface within the fluid domain is tracked using the Arbitrary Lagrangian Eulerian (ALE) formulation, while the Navier-Stokes equation governs each fluid particle.

As previously discussed, the primary output of interest in this study is the estimated maximum hydraulic pressure over the "window zone" for each building. This can be expressed as:

$$\mathcal{M}(\mathbf{x}) \rightarrow \mathcal{D}_{k,max} \tag{2}$$

where, $\mathcal{M}(\cdot)$ is the CFD model, $\mathbf{x}$ is the vector of intensify measures and layout and geometrical parameters of neighboring buildings listed in Table 1, and $\mathcal{D}_{k,max}$ is the maximum hydraulic

pressure across the "window zone" for the k^{th} building in the model.

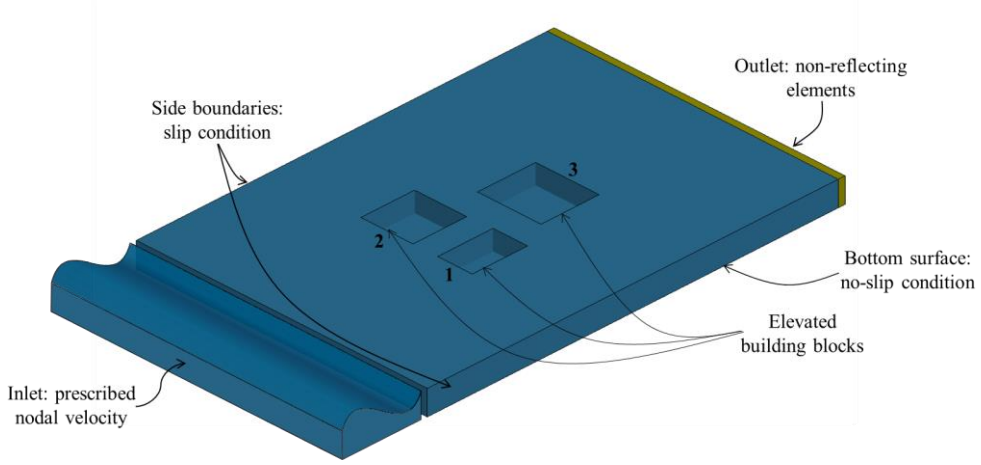

Figure 2: Numerical computational fluid dynamics (CFD) model including neighboring structures within the fluid domain

Developing a parameterized fragility model for a structure typically requires a sufficiently large dataset (on the order of thousands) representing different system parameter combinations and the associated failure-safe state of the structure [27]. In the present study, where the CFD analysis is leveraged to incorporate the effects of neighboring structures, such large computations become costly and time-consuming. Therefore, before the parameterized fragility model development, a surrogate model is derived that replaces the expensive CFD model while still providing reliable estimates of the (modified) hydraulic demand $\widehat{\mathcal{D}}_{k,max}$ to accelerate the estimation process. Accordingly, the next step provides details on the development of surrogate models.

2.2 Computationally efficient development of surrogate model using active learning

The objective of the surrogate model (denoted here as $\widehat{\mathcal{M}}_k(\cdot)$) is to replace the expensive numerical model ($\mathcal{M}(\mathbf{x})$) and provide accelerated estimation of demand ($\widehat{\mathcal{D}}_{k,max}$) while deriving the parameterized fragility model. However, when numerical model simulations are highly computationally expensive—as in the present study, where the CFD analysis of multiple structures in the fluid domain incurs substantial costs—developing a surrogate model also becomes challenging due to the significant requirement of computational resources and time. An active learning strategy is employed to overcome this challenge and expedite surrogate model development. Active learning can assist identifying samples of model input parameter combinations closer to the limit state classification boundary or exhibit higher errors in surrogate model predictions [20]. In essence, active learning guides the surrogate model training to include samples that improve performance, specifically on the limit state classification—a critical domain where accuracy is most needed for fragility derivation purposes. It is important to note that the algorithm of the machine learning tool used as a surrogate model remains unchanged based on the limit state criterion. Instead, the sample selection procedure is embedded to minimize computational costs during surrogate model training, guided by already defined limit state equation. The following steps outline the development of a surrogate model

implementing active learning, carried out separately for each building in the CFD model:

1. An experimental design set $\boldsymbol{X_1}$ of total sample size 300 is generated using Latin-hypercube sampling [28] to generate different parameter combinations of hazard intensity measures and spatial layout and geometrical parameters.
2. A dozen of samples are randomly sampled from $\boldsymbol{X_1}$ and are included in the initial sample set $\boldsymbol{\mathcal{I}}$. CFD simulations are employed to estimate $\mathcal{D}_{k,max}$ for each sample in set $\boldsymbol{\mathcal{I}}$.
3. Surrogate model $\widehat{\mathcal{M}}_k(\mathbf{x})$ is trained using dataset pair $\{\boldsymbol{\mathcal{I}}, \boldsymbol{\mathcal{D}_{k,max}}\}$ using a machine learning model. Gaussian Process Regression (GPR) is used here as the machine learning model given its popularity in active learning methods due to its capability of providing errors in the prediction (in terms of standard deviation of the prediction) along with its mean prediction estimate, and its flexibility through use of different kernels.
4. The developed surrogate model $\widehat{\mathcal{M}}_k(\mathbf{x})$ from previous step is employed on entire sample set $\boldsymbol{X_1}$ to obtain $\widehat{\boldsymbol{\mathcal{D}}}_{\boldsymbol{k,max}}$ and the corresponding standard deviation $\boldsymbol{\sigma}_{\widehat{\mathcal{D}}_{k,max}}$ of the prediction.
5. Using the surrogate model prediction from the previous step, limit state evaluation is performed for each sample in $\boldsymbol{X_1}$ using Equation 1.
6. Next, the learning function $L(\mathbf{X})$ is calculated which steers the sample selection process and is formulated as [20]:

$$L(\mathbf{X}) = \frac{\left|\hat{\mathcal{G}}(\mathbf{X})\right|}{\sigma_{\widehat{\mathcal{D}}_{k,max}}(\mathbf{X})} \tag{3}$$

   where, $\hat{\mathcal{G}}(\mathbf{X})$ is the limit state evaluated using mean $\widehat{\boldsymbol{\mathcal{D}}}_{\boldsymbol{k,max}}$ obtained from $\widehat{\mathcal{M}}_k(\mathbf{x})$. From Equation 3, a lower value of the learning function indicates that the sample is either close to the limit state classification boundary or yielding higher prediction errors. Intuitively, the sample with the lowest value of the learning functions can be termed as the "critical" sample $\mathbf{x}^*$.
7. If $L(\mathbf{x}^*) \geq 2$, the mean prediction is at least 2 standard deviations farther from the limit state classification boundary. This corresponds to a probability of misclassification of 0.023 [20]. Hence, this is considered as the stopping criterion, and the surrogate model training is stopped after this step. However, if $L(\mathbf{x}^*) < 2$, sample $\mathbf{x}^*$ is added to the set $\boldsymbol{\mathcal{I}}$ and the CFD analysis is performed to obtain its corresponding demand $\mathcal{D}_{k,max}$. The algorithm goes back to step 3 and the process repeats.

The number of samples required to train $\widehat{\mathcal{M}}_k(\mathbf{x})$ through this process are 53, 36, and 79, for building 1, building 2 and building 3, respectively. In total, the number of unique samples analyzed from $\boldsymbol{X_1}$ accounts for 32.33% (97 samples) of the total sample size, highlighting a substantial reduction in computational cost achieved during the development of surrogate models. Subsequently, developed surrogate models $\widehat{\mathcal{M}}_k(\mathbf{x})$ are used to derive topology-aware parameterized fragility models, as outlined in the next section.

2.3 Topology-aware parameterized fragility model development

The topology-aware parameterized fragility models are developed by conditioning the estimate of failure probability on spatial layout parameters of a building, along with parameters of hazard intensity measures. Given the closed-form functional expressions of the logistic regression model [29], it is used to develop topology-aware parameterized fragility models.

Accordingly, the parameterized fragility models have the following formulation:

$$P_k(\mathcal{G}_k(\mathbf{x}) < 0|\mathbf{x}) = P_{f,k} = \frac{1}{1 + \exp[-l_k(\mathbf{x})]} \tag{4}$$

where, $P_k(\mathcal{G}_k(\mathbf{x}) < 0|\mathbf{x})$ is the probability of failure (also denoted as $P_{f,k}$) for k^{th} building given the vector of input parameters $\mathbf{x}$, and $l_k(\mathbf{x})$ is a function containing polynomial terms of $\mathbf{x}$ along with model estimated coefficients.

The parameterized fragility model development begins with generating a larger experimental design set $\boldsymbol{\mathcal{X}}$ consisting of 50,000 samples using the Latin-hypercube sampling strategy to comprehensively cover the different parameter combinations for parameters in Table 1. The developed surrogate models $\widehat{\mathcal{M}}_k(\mathbf{x})$ enable rapid prediction of $\widehat{\mathcal{D}}_{k,max}$ for each sample in $\boldsymbol{\mathcal{X}}$. Subsequently, the limit state evaluation (Equation 1) is performed for each sample in $\boldsymbol{\mathcal{X}}$ to classify each sample as a failure or survival case (considering window failure). The classification of each sample is stored in a binary vector $\mathbf{b}_{\boldsymbol{k}}$, with 1 representing failure case and 0 representing survival. Finally, the dataset pair $\{\boldsymbol{\mathcal{X}}, \mathbf{b}_{\boldsymbol{k}}\}$ is used for training the topology-aware parameterized fragility model, which has the formulation shown in Equation 4.

Table 2: Performance of the developed topology-aware parameterized fragility models on test dataset

	Precision	Recall	F1-score	accuracy
Building 1	0.99	0.99	0.99	0.99
Building 2	0.99	0.99	0.99	0.99
Building 3	0.95	0.95	0.95	0.96

The $\{\boldsymbol{\mathcal{X}}, \mathbf{b}_{\boldsymbol{k}}\}$ dataset is split into two sets: 90% of the dataset is used for training, and 10% of the dataset is reserved for testing the model performance. Table 2 shows the performance of topology-aware parameterized fragility models evaluated using different metrics of confusion-matrix, and the model estimated expressions of $l_k(\mathbf{x})$ are:

$$\begin{aligned}
l_1(\mathbf{x}) &= -40.35 + 9.13S + 10.88H_w + 0.14\,T_w + 1.40U - 0.002L_w + 0.01d_X + 0.001d_Y \\
&\quad + 0.01e + 0.06b_1 + 0.01l_1 - 0.01b_2 - 0.01l_2 + 0.07b_3 - 0.008l_3 \\
l_2(\mathbf{x}) &= -43.38 + 9.77S + 12.67H_w + 0.01\,T_w + 0.42U + 0.03L_w + 0.002d_X + 0.001d_Y \\
&\quad - 0.003e + 0.05b_1 + 0.003l_1 - 0.0004b_2 - 0.004l_2 + 0.01b_3 + 0.06l_3 \\
l_3(\mathbf{x}) &= -15.90 + 3.56S + 2.55H_w - 0.02\,T_w + 0.51U + 0.047L_w - 0.0003d_X + 0.049d_Y \\
&\quad - 0.014e - 0.01b_1 + 0.02l_1 + 0.02b_2 - 0.09l_2 + 0.01b_3 - 0.001l_3
\end{aligned} \tag{5}$$

3 DISCUSSIONS

To highlight both types of effects of neighboring structures—shielding and channeling—fragility curves conditioned on the surge height are generated using the developed topology-aware parameterized fragility models for the windows, while keeping other model parameters constant. Table 3 shows two cases of different layout parameters with constant hazard and building geometry parameters selected for demonstration purposes, and the fragility curves are shown in Figure 3 (a) and (b) along with a schematic sketch of building layouts.

Table 3: Parameters used to generate fragility curves based on developed topology-aware parameterized fragility models

Case 1	$H_w = 0.5 * S$ m, $T_w = 5$ s, $U = 1.0$ m/s, $L_w = 25$ m, $d_X = 40$ m, $d_y = 5$ m, $e = 7$ m, $b_1 = 20$ m, $l_1 = 15$ m, $b_2 = 20$ m, $l_2 = 15$ m, $b_3 = 10$ m, $l_3 = 15$ m
Case 2	$H_w = 0.25 * S$ m, $T_w = 5$ s, $U = 1.0$ m/s, $L_w = 50$ m, $d_X = 5$ m, $d_y = 40$ m, $e = 10$ m, $b_1 = 20$ m, $l_1 = 15$ m, $b_2 = 20$ m, $l_2 = 15$ m, $b_3 = 10$ m, $l_3 = 15$ m

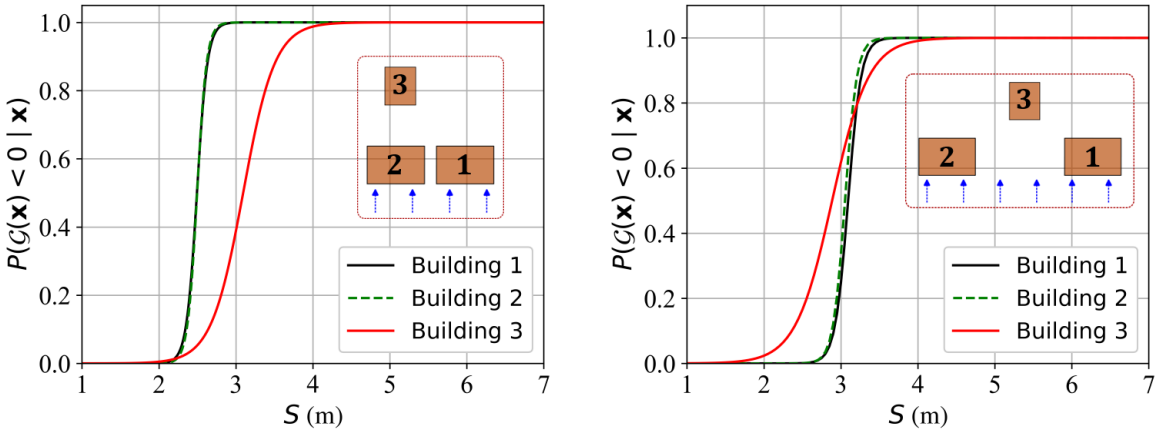

Figure 3: Fragility curves generated using parameters of (a) case 1 and (b) case 2, listed in Table 3

The parameters corresponding to case 1 represent shielding effects since the fragility curves show a reduction in the fragility of window damage for building 3 compared to building 1 and building 2, as can be observed from Figure 3 (a). Statistically, the median value of fragility (in terms of surge elevation) changes by 24.1% from building 1 (located in row 1) to building 3 (located in row 2), highlighting the importance of incorporating the effects of neighboring structures. Case 2 corresponds to the channeling effect for building 3, which shows an increase in fragility for window damage compared to buildings 1 and 2 (Figure 3 (b)). However, as the surge height increases, the channeling effects are diminished, and the failure probability differences converge as the hydrostatic loads due to surge height start dominating the window failure. These two examples highlight the substantial effects of neighboring structures on building fragility and showcase the importance of considering the impact of neighboring structures in regional risk assessment studies.

4 CONCLUSION

Motivated to refine the regional risk assessment studies for dense coastal residential infrastructure, this study demonstrates computationally efficient methodology to develop topology-aware parameterized fragility models considering the effects of neighboring buildings. The impact of neighboring structures on demand modification under storm surge and wave loads is captured through physics-based numerical computational fluid dynamics (CFD) analyses, including the neighboring buildings in the fluid-analysis domain. Constraints on parameterized fragility model development imposed by computational cost of CFD analysis

due to the addition of neighboring buildings is alleviated through developing surrogate models to accelerate the fragility derivation process. The development of surrogate models is guided through the component limit state function using an active learning strategy to further reduce the computational cost of developing surrogate models itself as it relies on CFD analysis.

To illustrate the proposed methodology, topology-aware parameterized fragility models are developed for one component of the building, i.e., windows. The fragility estimates derived for two example scenarios highlight the pronounced significance of neighboring buildings on fragility modification. As such, future studies will extend this work to develop parameterized fragility models for other failure modes and components, along with other design details and configurations of residential buildings to refine regional risk assessment studies.

ACKNOWLEDGEMENT

The authors would like to acknowledge the support of this research by the National Science Foundation (NSF) under award number CMMI-2227467. Any opinions, findings, and conclusions, or recommendations expressed in this paper are those of the authors and do not necessarily reflect the views of the sponsors.

REFERENCES

[1] NOAA National Centers for Environmental Information (NCEI), "U.S. Billion-Dollar Weather and Climate Disasters." 2025. doi: 10.25921/stkw-7w73.

[2] A. Hatzikyriakou and N. Lin, "Assessing the Vulnerability of Structures and Residential Communities to Storm Surge: An Analysis of Flood Impact during Hurricane Sandy," *Front. Built Environ.*, vol. 4, p. 4, Feb. 2018, doi: 10.3389/fbuil.2018.00004.

[3] A. Kennedy *et al.*, "Building Destruction from Waves and Surge on the Bolivar Peninsula during Hurricane Ike," *J. Waterway, Port, Coastal, Ocean Eng.*, vol. 137, no. 3, pp. 132–141, May 2011, doi: 10.1061/(ASCE)WW.1943-5460.0000061.

[4] A. Hatzikyriakou, N. Lin, J. Gong, S. Xian, X. Hu, and A. Kennedy, "Component-Based Vulnerability Analysis for Residential Structures Subjected to Storm Surge Impact from Hurricane Sandy," *Nat. Hazards Rev.*, vol. 17, no. 1, p. 05015005, Feb. 2016, doi: 10.1061/(ASCE)NH.1527-6996.0000205.

[5] T. Tomiczek, A. Kennedy, and S. Rogers, "Collapse Limit State Fragilities of Wood-Framed Residences from Storm Surge and Waves during Hurricane Ike," *J. Waterway, Port, Coastal, Ocean Eng.*, vol. 140, no. 1, pp. 43–55, Jan. 2014, doi: 10.1061/(ASCE)WW.1943-5460.0000212.

[6] T. Tomiczek *et al.*, "Hurricane Damage Classification Methodology and Fragility Functions Derived from Hurricane Sandy's Effects in Coastal New Jersey," *J. Waterway, Port, Coastal, Ocean Eng.*, vol. 143, no. 5, p. 04017027, Sep. 2017, doi: 10.1061/(ASCE)WW.1943-5460.0000409.

[7] T. Q. Do, J. W. Van De Lindt, and D. T. Cox, "Hurricane Surge-Wave Building Fragility Methodology for Use in Damage, Loss, and Resilience Analysis," *J. Struct. Eng.*, vol. 146, no. 1, p. 04019177, Jan. 2020, doi: 10.1061/(ASCE)ST.1943-541X.0002472.

[8] M. S. Alam, A. R. Barbosa, M. H. Scott, D. T. Cox, and J. W. Van De Lindt, "Development of Physics-Based Tsunami Fragility Functions Considering Structural

Member Failures," *J. Struct. Eng.*, vol. 144, no. 3, p. 04017221, Mar. 2018, doi: 10.1061/(ASCE)ST.1943-541X.0001953.

[9] C. Tarbotton, F. Dall'Osso, D. Dominey-Howes, and J. Goff, "The use of empirical vulnerability functions to assess the response of buildings to tsunami impact: Comparative review and summary of best practice," *Earth-Science Reviews*, vol. 142, pp. 120–134, Mar. 2015, doi: 10.1016/j.earscirev.2015.01.002.

[10] G. Hou, J. Wang, and A. Layton, "Numerical Methods for Fluid-Structure Interaction — A Review," *Commun. comput. phys.*, vol. 12, no. 2, pp. 337–377, Aug. 2012, doi: 10.4208/cicp.291210.290411s.

[11] C. Bernier and J. E. Padgett, "Fragility and risk assessment of aboveground storage tanks subjected to concurrent surge, wave, and wind loads," *Reliability Engineering & System Safety*, vol. 191, p. 106571, Nov. 2019, doi: 10.1016/j.ress.2019.106571.

[12] H. Park, T. Do, T. Tomiczek, D. T. Cox, and J. W. Van De Lindt, "Numerical modeling of non-breaking, impulsive breaking, and broken wave interaction with elevated coastal structures: Laboratory validation and inter-model comparisons," *Ocean Engineering*, vol. 158, pp. 78–98, Jun. 2018, doi: 10.1016/j.oceaneng.2018.03.088.

[13] M. Amini, D. Cox, A. Barbosa, and S. Appleton Figueira, "An integrated Pre and Post Storm Dataset for Hurricane Ian (2022)." Virtual Damage Assessment and First-floor Elevation Estimation: Application to Fort Myers Beach, Florida and Hurricane Ian (2022), DesignSafe-CI, 2024. [Online]. Available: https://doi.org/10.17603/ds2-c1g8-qy41

[14] S. A. Figueira, M. Amini, D. T. Cox, and A. R. Barbosa, "Methodology for Virtual Damage Assessment and First-Floor Elevation Estimation: Application to Fort Myers Beach, Florida and Hurricane Ian (2022)," *Nat. Hazards Rev.*, vol. 26, no. 2, p. 04025012, May 2025, doi: 10.1061/NHREFO.NHENG-2310.

[15] J. P. Moris, A. B. Kennedy, and J. J. Westerink, "Tsunami wave run-up load reduction inside a building array," *Coastal Engineering*, vol. 169, p. 103910, Oct. 2021, doi: 10.1016/j.coastaleng.2021.103910.

[16] Y. Nouri, I. Nistor, D. Palermo, and A. Cornett, "Experimental Investigation of Tsunami Impact on Free Standing Structures," *Coastal Engineering Journal*, vol. 52, no. 1, pp. 43–70, Mar. 2010, doi: 10.1142/S0578563410002117.

[17] S. Thomas, J. Killian, and K. Bridges, "Influence of Macroroughness on Tsunami Loading of Coastal Structures," *J. Waterway, Port, Coastal, Ocean Eng.*, vol. 141, no. 1, p. 04014028, Jan. 2015, doi: 10.1061/(ASCE)WW.1943-5460.0000268.

[18] T. Tomiczek, A. Prasetyo, N. Mori, T. Yasuda, and A. Kennedy, "Physical modelling of tsunami onshore propagation, peak pressures, and shielding effects in an urban building array," *Coastal Engineering*, vol. 117, pp. 97–112, Nov. 2016, doi: 10.1016/j.coastaleng.2016.07.003.

[19] A. O. Winter *et al.*, "Tsunami-Like Wave Forces on an Elevated Coastal Structure: Effects of Flow Shielding and Channeling," *J. Waterway, Port, Coastal, Ocean Eng.*, vol. 146, no. 4, p. 04020021, Jul. 2020, doi: 10.1061/(ASCE)WW.1943-5460.0000581.

[20] B. Echard, N. Gayton, and M. Lemaire, "AK-MCS: An active learning reliability method combining Kriging and Monte Carlo Simulation," *Structural Safety*, vol. 33, no. 2, pp. 145–154, Mar. 2011, doi: 10.1016/j.strusafe.2011.01.002.

[21] M. Moustapha, S. Marelli, and B. Sudret, "Active learning for structural reliability: Survey, general framework and benchmark," *Structural Safety*, vol. 96, p. 102174, May 2022, doi: 10.1016/j.strusafe.2021.102174.
[22] C. Dawson, "Simulation Data of Storm Surge and Waves for Historical Hurricanes in the Gulf of Mexico." Hurricane Surge and Wave Data for Engineering Analysis, DesignSafe-CI, 2023. [Online]. Available: https://doi.org/10.17603/ds2-nqxf-3g65
[23] Microsoft, "Worldwide building footprints derived from satellite imagery." 2025. [Online]. Available: https://github.com/microsoft/GlobalMLBuildingFootprints
[24] K. Gurley, J. P. Pinelli, C. Subramanian, A. Cope, L. Zhang, and J. Murphree, "Predicting the vulnerability of typical residential buildings to hurricane damage," Miami: I.H.R. Center, Florida International Univ, 2005.
[25] Ansys, *LS-Dyna*. (2023). Ansys.
[26] J. D. Fenton, "Use of the programs FOURIER, CNOIDAL and STOKES for steady waves," 2015.
[27] R. Rincon and J. E. Padgett, "Fragility modeling practices and their implications on risk and resilience analysis: From the structure to the network scale," *Earthquake Spectra*, vol. 40, no. 1, pp. 647–673, Feb. 2024, doi: 10.1177/87552930231219220.
[28] M. D. Mckay, R. J. Beckman, and W. J. Conover, "A Comparison of Three Methods for Selecting Values of Input Variables in the Analysis of Output From a Computer Code," *Technometrics*, vol. 42, no. 1, pp. 55–61, Feb. 2000, doi: 10.1080/00401706.2000.10485979.
[29] D. W. Hosmer Jr, S. Lemeshow, and R. X. Sturdivant, *Applied logistic regression*. John Wiley & Sons, 2013.